

# Soft Matter

Accepted Manuscript



This is an *Accepted Manuscript*, which has been through the Royal Society of Chemistry peer review process and has been accepted for publication.

*Accepted Manuscripts* are published online shortly after acceptance, before technical editing, formatting and proof reading. Using this free service, authors can make their results available to the community, in citable form, before we publish the edited article. We will replace this *Accepted Manuscript* with the edited and formatted *Advance Article* as soon as it is available.

You can find more information about *Accepted Manuscripts* in the [Information for Authors](#).

Please note that technical editing may introduce minor changes to the text and/or graphics, which may alter content. The journal's standard [Terms & Conditions](#) and the [Ethical guidelines](#) still apply. In no event shall the Royal Society of Chemistry be held responsible for any errors or omissions in this *Accepted Manuscript* or any consequences arising from the use of any information it contains.

## ARTICLE

# Modulation of friction dynamics in water by changing the combination of the loop- and graft-type poly(ethylene glycol) surfaces

Cite this: DOI: 10.1039/x0xx00000x

Received 00th January 2014,  
Accepted 00th January 2014

DOI: 10.1039/x0xx00000x

[www.rsc.org/](http://www.rsc.org/)

Ji-Hun Seo,<sup>a†</sup> Yusuke Tsutsumi,<sup>b†</sup> Akinori Kobari,<sup>c</sup> Masayuki Shimojo,<sup>c</sup> Takao Hanawa,<sup>b</sup> and Nobuhiko Yui,<sup>a\*</sup>

A Velcro-like poly(ethylene glycol) (PEG) interface was prepared in order to control the friction dynamics of material surfaces. Graft- and loop-type PEGs were formed on mirror-polished Ti surfaces using an electrodeposition method with mono- and di-amine functionalized PEGs. The friction dynamics of various combinations of PEG surfaces (i.e., graft-on-graft, loop-on-loop, graft-on-loop, and loop-on-graft) were investigated by friction testing. Here, only the Velcro-like combinations (graft-on-loop and loop-on-graft) exhibited a reversible friction behavior (i.e., reset of kinetic friction coefficient and reappearance of maximum static friction coefficient) during the friction tests. The same tendency was observed when the molecular weights of loop- and graft-type PEG were tested at 1 k and 10 k, respectively. This indicates that a Velcro-like friction behavior could be induced by simply changing the conformation of PEGs, which suggests a novel concept of altering polymer surfaces for effective control of friction dynamics.

## Introduction

Velcro has been widely recognized in the textile industry as well as the aerospace industry as a trade name for a hook-and-loop fastener inspired by the burdock burr because of its fascinating mechanism of reversible attachment–detachment between two facing fabrics.<sup>1</sup> The fibrous entanglement between two hook- and loop-like fabric surfaces is a key mechanism for revealing reversible and reproducible attachment. Similar conformation-dependent interfacial phenomena are also present in biological environments. In the field of orthopedics, it has been well established that the lubrication of articular cartilage is governed by the conformational change of lubricin, a mucin-like proteoglycan found in synovial fluid.<sup>2, 3</sup> Various case

studies showed that loop- or tail-like conformational states of proteoglycan on materials surfaces with different polarity have a considerable effect on their friction coefficients.<sup>4</sup> It has been suggested that the tail-like conformation of the proteoglycan readily induces a heightened form of molecular interaction such as hyaluronic-acid-based electrostatic interaction or physical entanglement of surface molecules, thus leading to a higher friction coefficient compared to the loop-like conformation.<sup>5</sup> Although the mechanism is slightly different, both cases provide inspiration for the design of a functional interface capable of modulating friction dynamics (i.e., conformation-dependent friction control). By adopting Velcro's mechanism of reversible attachment and detachment, the reversible friction behavior, that is, the reset of kinetic friction coefficient and reappearance of the maximum static friction coefficient, might be induced by simply changing the conformation of surface polymers. To demonstrate the feasibility of applying this bio-inspired interfacial phenomenon as a method of friction control, Velcro-like loop and hook surfaces were formed on a Ti substrate. This was accomplished by the electrodeposition method, which is a simple and robust means of immobilizing functional polymers on the surface of metallic materials by electrostatic interaction.<sup>6–8</sup> Similar to other types of physical immobilization of polymer materials (e. g., mediating hydrophobic anchoring groups),<sup>9,10</sup> electrodeposited polymers or oligopeptides containing positively charged amine groups

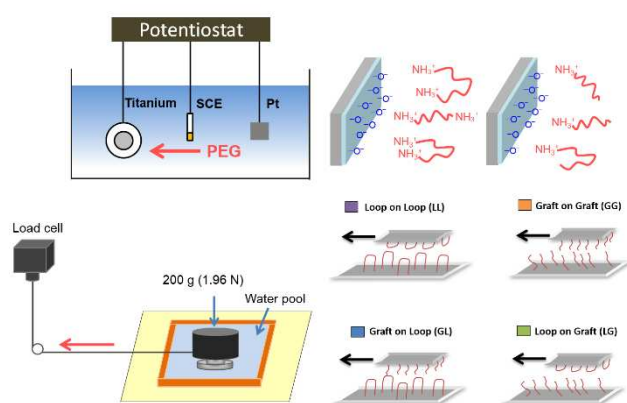
<sup>a</sup>Department of Organic Biomaterials, Institute of Biomaterials and Bioengineering, Tokyo Medical and Dental University, Tokyo 101-0062, Japan.

<sup>b</sup>Department of Metallic Biomaterials, Institute of Biomaterials and Bioengineering, Tokyo Medical and Dental University, Tokyo 101-0062, Japan.

<sup>c</sup>Graduate School of Engineering Science, Shibaura Institute of Technology, Tokyo 135-8548, Japan.

†These authors contributed equally.

\* Corresponding author: [yui.org@tmd.ac.jp](mailto:yui.org@tmd.ac.jp)



**Scheme 1.** Schematic illustration of the electrodeposition process, friction test, and the combination of graft- and loop-type PEG surfaces

can be stably immobilized on metallic materials, even for biomedical applications.<sup>11</sup>

In this research, mono-methoxy-terminated poly(ethylene glycol) (PEG) with an amine-functionalized end group was prepared for developing the graft-type surface, while di-amine-functionalized PEG was prepared for the loop-type surface. A conformation-dependent friction behavior was expected to occur by forming these bio-inspired Velcro-like polymer interfaces. Accordingly, the purpose of this study was to investigate whether the reversible friction behavior could be modulated by simply changing the surface conformations of anchored polymer chains.

## Results and Discussion

After the mono- or di-amine-functionalized PEGs were immobilized on Ti surfaces, the friction values between the two surfaces were characterized in comparison with loop-loop and tail-tail surfaces in aqueous medium, as depicted in Scheme 1. Previously, electrodeposition of various types of aminated polymers on Ti surfaces was successfully conducted by our group to prepare metallic-material-based functional biomedical devices.<sup>12,13</sup> In particular, it was established that polymers containing an aminated end group were more effectively immobilized on the surface by electrodeposition than those with an aminated side group in the polymer chain.<sup>14</sup> In this study, a molecular weight of 5 k was used for the mono- and di-amine end-functional PEGs (graft- and loop-type PEG surfaces, respectively). **Scheme 1** shows the overall concept for producing the graft- and loop-type PEG surfaces, and the following friction test. Aminated PEGs were protonated in alkaline buffer (pH 11), and electrodeposited on the Ti prescathode surface.

**Fig. 1** shows atomic force microscopy images for graft- and loop-like PEGs deposited on the Ti surface, taken in an aqueous medium. The mirror-polished Ti surface is clearly very flat, with low RMS roughness ( $< 1$  nm) prior to electrodeposition (**Fig. 1a**). When the Ti surface was cathodically polarized in alkaline buffer without PEGs, a minor dissolution process progressed for 15 min on the Ti surface, and a concave morphology was observed on the treated surfaces. Although the surface morphology was no longer extremely flat, the roughness of the surface remained very low (less than 5 nm). This indicates that the conditions of electrodeposition are favorable for eliminating the effects of surface roughness of Ti

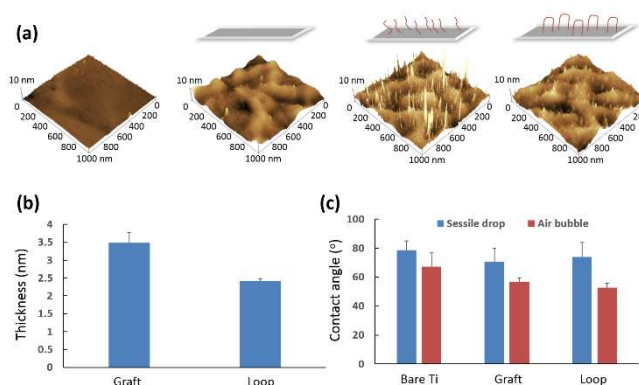


**Fig. 1** (a) AFM images of Ti surfaces. From left to right: mirror-polished Ti, electrochemically treated bare Ti without PEG, graft-type PEG, and loop-type PEG-immobilized Ti surfaces. (b) Thickness of a PEG (5 k) immobilized surface. (c) Water and air bubble contact angles measured in dry and wet states, respectively.

on friction dynamics. The mirror-polished Ti was then electrochemically treated with mono- or di-amine functionalized PEG-containing alkaline buffer, and the morphologies were also analyzed by means of atomic force microscopy (AFM). As a result, the mono-amine functionalized PEG-treated surface exhibited a rough and brush-like morphology, in addition to the concave morphology of Ti substrate. In contrast, the di-amine functionalized PEG-treated surface had a small, bump-like morphology on the concave Ti substrate. This is probably due to the different conformation of immobilized PEG on the Ti surface. Because both mono- and di-amine functionalized PEGs have the same molecular weight, this higher surface roughness of graft-type surfaces is thought to be caused by higher chain mobility of the immobilized PEG in hydration states. A similar tendency was also observed when the thickness of immobilized PEG was analyzed using ellipsometry. As shown in **Fig. 1**, the graft-type PEG surface shows a greater thickness than the loop-type one, which may also be attributed to the different conformation of the graft- and loop-type PEG surfaces. The change in surface properties induced by PEG electrodeposition was analyzed in terms of the wettability to water. **Fig. 1** also shows the results of contact-angle measurements in dried and wet states by means of sessile water-drop or air-bubble contact, respectively. As shown, both graft- and loop-type surfaces show a slightly reduced contact angle in both types of measurement. This indicates that the polarity of the Ti surface was successfully modified by the immobilization of hydrophilic PEG chains.

Friction behavior at the interface between PEG-immobilized Ti surfaces was estimated in four different combinations, as depicted in Scheme 1. To demonstrate the formation of Velcro-like molecular entanglement, different sets of interface, such as loop-on-loop (LL) and graft-on-graft, were prepared as control surfaces in addition to the graft-on-loop (GL) and loop-on-graft (LG) combinations. **Fig. 2** shows the results of static-friction-coefficient measurements from twenty repeated friction tests conducted on the same surface. As shown, the combination of non-treated Ti surfaces (BB) shows a 0.4–0.5 value for the static friction coefficient ( $\mu_s$ ). Similar values of  $\mu_s$  were observed with the LL combination. This indicates that the LL combination could not induce significant molecular entanglement to have an effect on the friction behavior at the

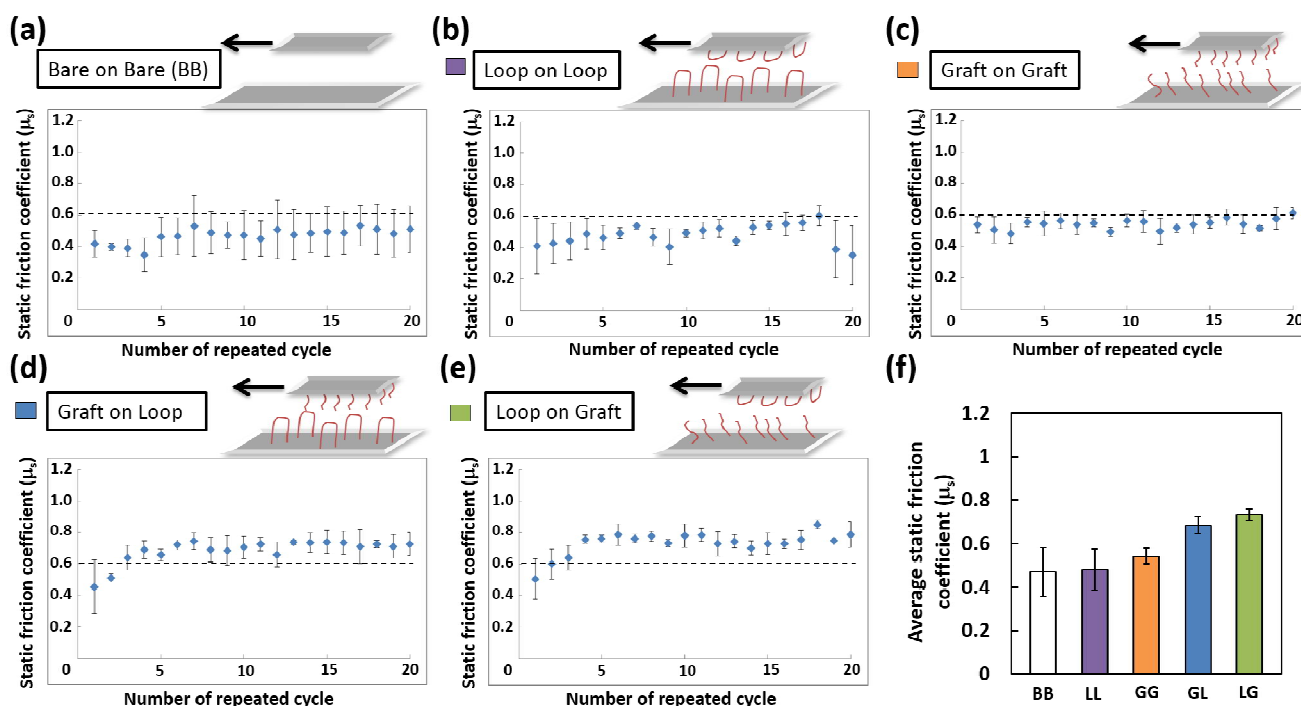


**Fig. 2** Static friction coefficient of (a) bare-on-bare, (b) loop-on-loop, (c) graft-on-graft, (d) graft-on-loop, and (e) loop-on-graft combinations measured during twenty repeated friction tests. (f) Average friction coefficient for each combination.

interfaces. The  $\mu_s$  values for the GG combination seemed slightly higher (ca. 0.05) than the BB or LL combinations, but the difference was within a reasonable error. The value of  $\mu_s$  is greatly dependent on physicochemical properties (density, surface roughness, polarity, etc.) of the materials' surfaces.<sup>15–17</sup> In particular, the polarity of polymer-immobilized surfaces has been posited as a key factor dominating the friction behavior of material surfaces in aqueous media, due to the lubricating effect of the hydration layer forming around the polar chemical groups.<sup>18</sup> For this reason, hydrophilic polymers such as PEG or poly(2-hydroxyethyl methacrylate) have been incorporated into various materials surfaces with the intent of decreasing the friction coefficient.<sup>19–21</sup> However, in this study, no significant changes to  $\mu_s$  values were observed for the LL and GG combinations, even though both surfaces reveal a slightly heightened hydrophilic property when compared to bare Ti. This is possibly caused by the compensation effect of the increased surface roughness due to PEG immobilization. Although this immobilization slightly increases the hydrophilicity of the Ti surface, the surface roughness was also greatly increased, as shown in the AFM images. This increased surface roughness of graft-type PEG surfaces is likely to result in slightly higher  $\mu_s$  values for the GG combination than the LL one, within a reasonable error. The effect of molecular entanglement on the increase of  $\mu_s$  was maximized when two different PEG surfaces were combined (i.e., the GL and LG combinations). As shown in **Fig. 2**, the  $\mu_s$  values for the GL and LG combinations were within 0.7–0.8, which is higher than for the GG (rough surfaces) combination. Because the increased  $\mu_s$  values are thought to be owing to the molecular entanglement induced by PEG chains, it could be hypothesized that much stronger molecular entanglements are generated

when graft- and loop-type surfaces are combined with each other.

To more clearly understand the interfacial phenomenon, a real-time change in the friction coefficient was monitored according to sample displacement (**Fig. 3**). Here, the non-treated Ti surface shows the typical friction dynamics of a flat surface (i.e., maximized  $\mu_s$  followed by constant  $\mu_k$  as a function of time).<sup>22</sup> For the LL combination, the linear and constant  $\mu_k$  were slightly altered, exhibiting a serrated profile. The change was more pronounced for the rough surface combination (GG), which is possibly due to the continuous entanglement and dissociation cycles between immobilized PEG molecules as the samples were dragged. Although both the LL and GG combination show different friction dynamics compared with the flat Ti surface, both surfaces still oscillate above the minimum  $\mu_k$  values (dash line) during the measurement. This indicates that both LL and GG combinations maintain a typical friction behavior (i.e., the sample was continuously sliding while maintaining a certain level of  $\mu_k$ ). Contrary to this, a drastic change in the kinetic friction dynamics was observed for the GL and LG combinations. In both cases, at least one zero-set point for  $\mu_k$  (arrow) was observed during the measurement, and this phenomenon was observed throughout repeated testing. An interesting point here is the reappearance of the maximized  $\mu_s$  right after the zero-set point, and this process seems to indicate a reproduction of the initial friction behavior. That is, conversely to the continuous molecular entanglement of graft-graft chain interactions in the GG combination, this mixed combination of GL and LG seem to reset to reproduce the initial friction behavior of the interfaces. This indicates that the sliding samples temporally halt their movement and once again experience a  $\mu_s$  before restarting movement. Since these graft-

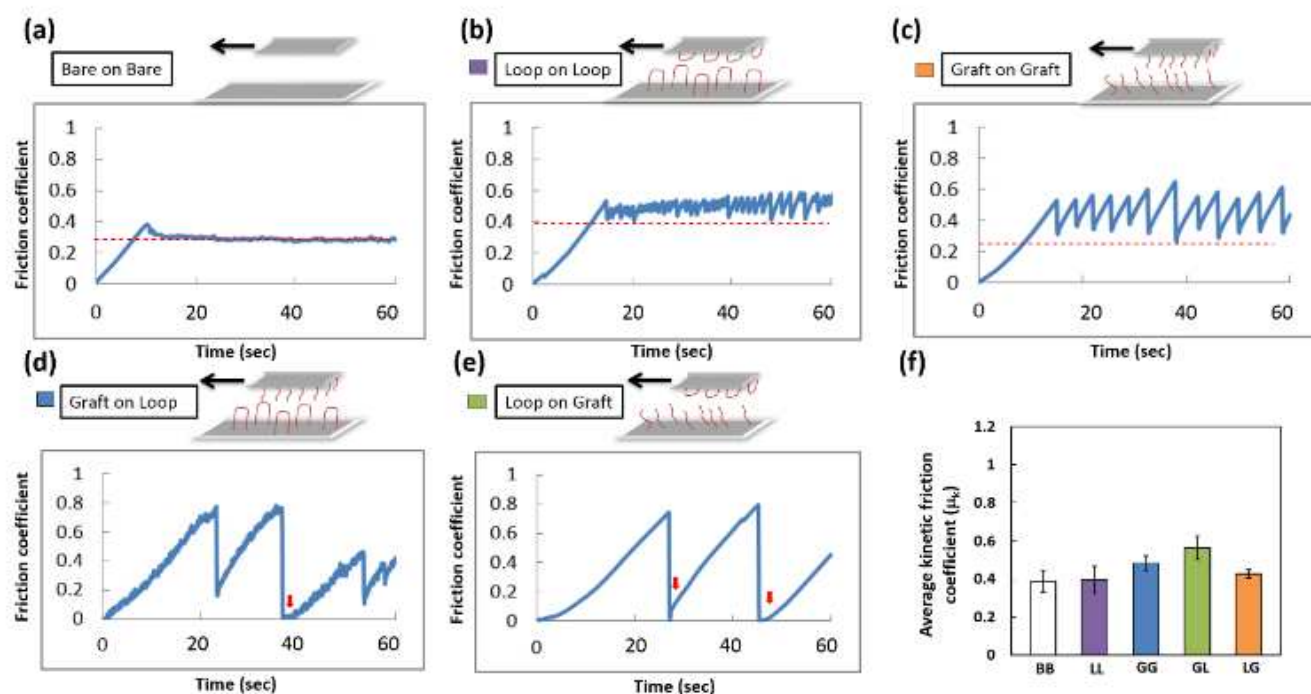


**Fig. 3** Kinetic friction behavior of (a) bare on bare, (b) loop on loop, (c) graft on graft, (d) graft on loop, and (e) loop on graft combinations during the friction tests. (3 mm/min) Dash line indicates the minimum friction coefficient maintained during the test. The arrows indicate the zero-set point during the friction test. (f) Average kinetic friction coefficient of each combination.

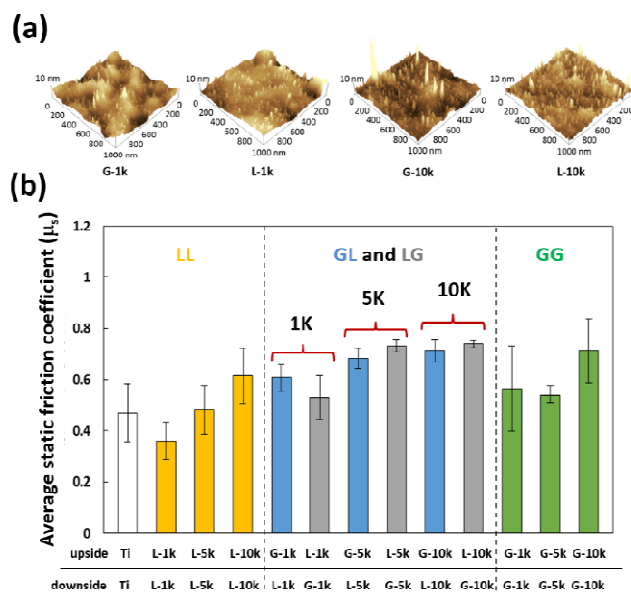


**Fig. 4** (a) AFM images of graft- and loop-type surfaces prepared with PEG of molecular weights 1 k and 10 k, respectively. (b) Average static friction coefficient for each combination.

and loop-type combinations are inspired by the molecular mechanism of the burdock burr, we speculate that the reversible friction behavior is induced by repeated temporal molecular entanglement of graft-type PEG into loop-type PEG.

To establish the effect of molecular weight of immobilized PEG on friction dynamics, the same friction tests were conducted after immobilizing mono- or di-amine functionalized PEGs with molecular weights of 1 k and 10 k, respectively. The same morphology as the rough graft-type and round loop-type surfaces were seen on the resulting PEG-immobilized surfaces (Fig. 4a), which indicates that the graft- and loop-type PEG surfaces with different molecular weights were successfully produced via electrodeposition. Fig. 4b shows the resulting maximum  $\mu_s$  values for each combination with different molecular weights. As shown, the maximum  $\mu_s$  gradually increased with molecular weight in all combinations. This indicates that the static friction coefficient is also dependent on the molecular weight of the immobilized polymer chains. Because the longer chain length might induce a stronger molecular entanglement,<sup>23</sup> the increased  $\mu_s$  value with higher molecular weight is thought to be due to the increased molecular entanglement. For the case of 1 k molecular weights, the maximum  $\mu_s$  value increased when the graft- and loop-type surface (GL and LG) were combined with each other, as with 5 k weights. This indicates that when low-molecular-weight PEGs ( $\leq 5$  k) are immobilized on a Ti surface, molecular conformation is very important in controlling the maximum value of  $\mu_s$ . In the case of 10 k molecular weights, the maximum  $\mu_s$  value was not significantly increased with GL and LG combinations compared to LL and GG ones. Because this molecular weight might induce significant molecular entanglement, even in the LL and GG combinations, owing to the long chain length, we expect that only a limited conformational effect occurs in the GL and LG combinations. The kinetic friction behavior was also monitored for each combination at different molecular weights, and the results are displayed in Fig. 5. Although only a limited effect of the GL

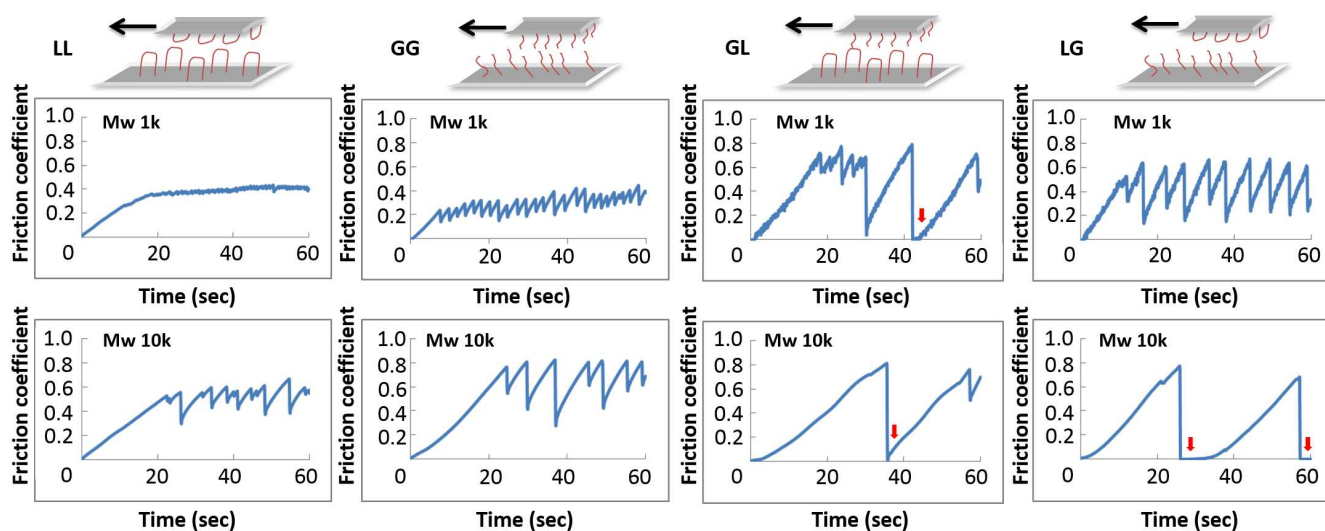


**Fig. 5** Kinetic friction of (from left) loop-on-loop, graft-on-graft, graft-on-loop, and loop-on-graft combinations prepared with two different PEGs (1 k and 10 k) during the friction tests. (3 mm/min)

and LG combination on the maximum  $\mu_s$  value was observed, the kinetic friction behavior was greatly affected by graft- and loop-type combinations, independent of the molecular weights. For the GL combination, the zero-set point was once again observed for both molecular weights. This indicates that molecular entanglement could be effectively induced in GL combinations for a wide range of molecular weights. In the case of LG combination, the zero-set point was also observed on the 10 k surface, which indicates that molecular entanglement could be stably induced in a high-molecular-weight region when graft- and loop-type surfaces were combined with each other. In contrast, we could not observe the zero-set point for the LG combination with a 1 k surface, even after three reproducing tests of twenty repetitions each. Although the mechanism here is not yet clearly understood, the combination of sliding loop to fixed graft is thought to barely form a molecular entanglement when the chain length is so short (i.e., 1 k).

To affect a polymer-chain-induced friction behavior, the same friction tests were conducted after adding bovine serum albumin (BSA) in aqueous medium. Here, we confirmed that the observed increase in the  $\mu_s$  value in GL and LG combinations could be cancelled by adding BSA in the friction system (data not shown). This finding reiterates the notion that the friction behavior taking place at the interface between graft- and loop-type PEG surfaces is induced by a molecular entanglement. In any event, possibly the combination of graft- and loop-type PEG surfaces is an effective means for developing a functional interface with reversible friction behavior (like the burdock burr) at a molecular level, and this may lead to a novel regime of molecular-Velcro materials design for the control of friction dynamics.

## Conclusions

Velcro-inspired graft- and loop-type polymer surfaces were developed for the control of friction dynamics at the materials' interfaces. Graft- and loop-type PEG surfaces with different molecular weights were successfully developed by a simple electrodeposition method, and the key reversible-friction

behavior was successfully induced. This result demonstrates that by simply changing the surface conformation of the deposited polymers, the friction dynamics can be simply modulated on the materials' surfaces.

## Materials and Methods

### MATERIALS

Poly(ethylene glycol) (PEG) (5 k, 10 k) and PEG monomethyl ether (5 k, 10 k) were purchased from Sigma Aldrich Chemical Co. (St. Louis, MO, USA), and PEG 1 k was purchased from Alfa Aesar (Ward Hill, MA, USA). The hydroxyl terminal groups were converted to amine groups by a previously reported method.<sup>24</sup> Briefly, PEG 10 k (1 g, 0.1 mmol), dimethylaminopyridine (0.0366 g, 0.3 mmol), and triethylamine (0.0303 g, 0.3 mmol) were dissolved in 5 mL anhydrous dichloromethane and the mixture was placed in ice bath. To this, a solution of p-TsCl (0.0570 g, 0.3 mmol) in 5 mL anhydrous dichloromethane was slowly added and allowed to react overnight. The mixture was then diluted with a NaHCO<sub>3</sub> (Wako Chemical Co., Tokyo, Japan) aqueous solution, and the organic layer was extracted and concentrated, followed by re-precipitation in diethyl ether to obtain tosylated PEG. The tosylated PEG was then dissolved in anhydrous DMF and mixed with excess potassium phthalimide (Wako). This mixture was then heated at 100°C overnight. After evaporating the DMF, the reactant was dispersed in chloroform. Then, after filtering the suspension, the organic solution was re-precipitated in diethyl ether to obtain phthalimide-functionalized PEG (PI-PEG). PI-PEG was dissolved in ethanol, and hydrazine (Wako) was injected into the solution. The mixture was then heated to 90°C, and refluxed overnight. After evaporating the solvent, the crude product was dissolved in dichloromethane, filtered, and re-precipitated in diethyl ether to obtain aminated PEGs.

The PEG monomethyl ether (1 k) p-toluenesulfonate purchased from Alfa Aesar (Ward Hill, MA, USA) was also aminated as described above.

<sup>1</sup>H nuclear magnetic resonance (NMR) measurement was conducted with Bruker Avance III 500 MHz spectrometer

(Bruker Biospin, Rheinstetten, Germany) in chloroform-*d* (Sigma Aldrich) to ensure the substitution of the end-functional PEGs in each synthetic step (> 90% yield).<sup>24</sup> Size exclusion chromatography (SEC) analysis was conducted using a JASCO RI-1530 detector containing two connected TSK-GEL,  $\alpha$ -4000 and  $\alpha$ -2500 gel columns (Tosoh Corp. Tokyo, Japan) with DMSO (10 mM LiBr) as an eluent at 37°C to ensure the molecular weight of 1k, 5k, and 10k of tosylated PEGs.

#### ELECTRODEPOSITION

PEG molecules were dissolved in a 0.3 mol L<sup>-1</sup> NaCl solution with a concentration of 1 wt%. Electrodeposition of PEG on Ti was performed using a potentiostat (HAB-151, Hokuto Denko Corp., Japan) connected with a function generator (WF1946B, NF Corp, Japan). After immersion in the PEG solution, the open circuit potential, OCP, of Ti versus saturated calomel electrode, SCE, was measured for 10 min. Thereafter, direct current by a cathodic potential was charged at -3 V and maintained for 30 min.

With a charging potential, PEG molecules dissolved in the solution were immobilized on the Ti electrode. After electrodeposition, specimens were rinsed in deionized water and dried with a stream of nitrogen gas (99.9%). The details of the electrodeposition system are described elsewhere.<sup>7</sup>

#### CONTACT ANGLE MEASUREMENT

The water and air bubble contact angle were measured using a goniometer (Kyowa Interface Science Co., Tokyo, Japan). On the dry surface, 3  $\mu$ L of water droplets were allowed to set for 30 s, and the contact angles were measured using a photographic image. The air-bubble contact angle was measured by producing 5  $\mu$ L of air bubbles to a water surface; this angle was also measured using a photographic image.

#### ELLIPSOMETRY

The apparent thickness of PEG layers immobilized on Ti by electrodeposition was determined with ellipsometry (DVA-36Ls, Mizojiri Optical Co., Ltd., Japan) in air. The light source was a He-Ne laser with a wavelength of 632.8 nm, and the incident angle to the surface of the specimen was 70°. The thickness was calculated using a refraction index (*n*) and an extinction coefficient (*k*) obtained from an original PEG-free Ti surface: the *n* and *k* of the Ti substrate were roughly 2.3 and 3.0, respectively.

#### ATOMIC FORCE MICROSCOPY

The morphology of PEG layer immobilized on Ti by electrodeposition was imaged in an aqueous medium with scanning probe microscopy (SPM, SPM-9600, SHIMADZU Corp., Japan) in the dynamic mode (non-contact mode). The image size was 1  $\times$  1  $\mu$ m

#### FRICTION TEST

The evaluation of static and dynamic friction coefficients was conducted using a tensile machine (AG-IS 500N, SHIMADZU Corp., Japan) following the ASTM Standard D-1894. The upper Ti specimen disk (15 mm in diameter) was forced to slide on the bottom Ti specimen (20 mm in diameter). Total load was adjusted to 1.96 N (200 gf) by a weight placed on the sliding specimen.

#### Acknowledgements

This work was supported by JSPS KAKENHI Grant Number 22240059 and Grant Number 25282142.

#### References

1. D. Kretschmann, *Nat. Mater.*, 2003, **2**, 775.
2. T. Pettersson, A. Dedinaite, *J. Colloid Interface Sci.*, 2008, **324**, 246.
3. D. P. Chang, N. I. Abu-Lail, F. Guilak, G. D. Jay, S. Zauscher, *Langmuir*, 2008, **24**, 1183.
4. J. M. Coles, D. P. Chang, S. Zauscher, *Curr. Opin. Colloid Interf. Sci.*, 2010, **15**, 406.
5. D. P. Chang, N. I. Abu-Lail, J. M. Coles, F. Guilak, G. D. Jay, S. Zauscher, *Soft Matter*, 2009, **5**, 3438.
6. Y. Tanaka, Y. Matsuo, T. Komiya, T. Komiya, Y. Tsutsumi, H. Doi, T. Yoneyama, T. Hanawa, *J. Biomed. Mater. Res. A*, 2010, **92A**, 350.
7. Y. Tanaka, H. Saito, Y. Tsutsumi, H. Doi, H. Imai, T. Hanawa, *Mater. Trans.*, 2008, **49**, 805.
8. Y. Tanaka, K. Matin, M. Gyo, A. Okada, Y. Tsutsumi, H. Doi, N. Nomura, J. Tagami, T. Hanawa, *J. Biomed. Mater. Res. A*, 2010, **95A**, 1105.
9. J.-H. Seo, S. Kakinoki, Y. Inoue, T. Yamaoka, K. Ishihara, N. Yui, *Soft Matter*, 2012, **8**, 5477.
10. J.-H. Seo, S. Kakinoki, Y. Inoue, T. Yamaoka, K. Ishihara, N. Yui, *J. Am. Chem. Soc.*, 2013, **135**, 5513.
11. K. Oya, Y. Tanaka, H. Saito, K. Kurashima, K. Nogi, H. Tsutsumi, Y. Tsutsumi, H. Doi, N. Nomura, T. Hanawa, *Biomaterials*, 2009, **30**, 1281.
12. T. Hanawa, *Jpn Dent. Sci. Rev.*, 2010, **46**, 93.
13. T. Hanawa, *Adv. Mater.*, 2012, **13**, 064102.
14. Y. Tanaka, H. Doi, Y. Iwasaki, S. Hiramoto, T. Yoneyama, K. Asami, H. Imai, T. Hanawa, *Mater. Sci. Eng. C*, 2007, **27**, 206.
15. W. R. Chang, I. Etsion, *J. Tribol.*, 1988, **110**, 57.
16. P. J. Blau, *Tribol. Inter.*, 2001, **34**, 585.
17. U. Raviv, S. Giasson, N. Kampf, J. F. Gohy, R. Jerome, J. Klein, *Nature*, 2003, **425**, 163.
18. S. Nagaoka, R. Akashi, *Biomaterials*, 1990, **11**, 419.
19. T. Drobek, N. D. Spencer, *Langmuir*, 2008, **24**, 1484.
20. T. Moro, Y. Takatori, K. Ishihara, T. Konno, Y. Takigawa, T. Matsushita, U.-I. Chung, K. Nakamura, H. Kawaguchi, *Nat. Mater.*, 2004, **3**, 829.
21. M. Kyomoto, T. Moro, S. Yamane, K. Watanabe, M. Hashimoto, Y. Takatori, S. Tanaka, K. Ishihara, *Biomaterials*, 2014, **35**, 6677.
22. V. I. Johannes, M. A. Green, C. A. Brockley, *Wear*, 1973, **24**, 381.
23. L. Leger, E. Raphael, H. Hervet, *Adv. Polym. Sci.*, 1999, **138**, 185.
24. S. Zalipsky, C. Gilon, A. Zilkha, *Eur. Polym. J.*, 1983, **19**, 1177.